The Endocranial Anatomy of Maba 1

Xiu-jie Wu[1] and Emiliano Bruner[2]*

[1]*Key Laboratory of Vertebrate Evolution and Human Origins, Institute of Vertebrate Paleontology and Paleoanthropology, Chinese Academy of Sciences, 100044 Beijing, China*
[2]*Grupo de Paleobiología, Centro Nacional de Investigación sobre la Evolución Humana, Paseo Sierra de Atapuerca 3, Burgos 09002, Spain*

KEY WORDS human evolution; paleoneurology; cranial anatomy; Asia; Middle-Late Pleistocene

ABSTRACT

Objectives: Maba 1, a partial cranium from Guandong Province (China) tentatively dated between 300 and 130 ka, has been suggested to display a mosaic of archaic and derived features, including facial affinities with Neandertals. This study aims to evaluate whether Maba 1 shows a derived endocranial phenotype, or if it displays a plesiomorphic braincase morphology.

Materials and methods: We analyzed a set of metric variables on fossil and modern human endocasts using bivariate correlation, principal component analysis, and cluster analyses, to evaluate the morphological affinities of the Maba 1 endocast.

Results: The cranial capacity, estimated at around 1300 cc, and the endocranial proportions of Maba 1 are within the ranges of modern humans, Neandertals and *Homo heidelbergensis*. However, the frontal lobes are narrow and the parietal areas are short and flattened, as in *H. heidelbergensis* and *H. erectus*. Nonetheless, the position of the frontal lobes relative to the orbits, the morphology of the frontal sinus and the curve of the frontal squama are more derived, being similar to Neandertals and modern humans.

Conclusions: The endocast displays a general archaic morphology, although with some derived features associated with the spatial relationships with the face. A similar admixture was described for other Middle Pleistocene samples, like Sima de los Huesos. Future phylogenetic studies must re-evaluate the facial skeleton to consider whether its features can be considered as related to the Neandertal lineage. Alternatively, they should be interpreted as the result of homoplasy and parallelism within the genus *Homo*, and may reflect a predominantly Asian variation. Am J Phys Anthropol 000:000–000, 2016.

Since its discovery in 1958 in the Maba village (Guangdong Province, China), the taxonomic and phylogenetic position of the Maba 1 human fossil has been a source of debate (Wu, 1988; Schwartz and Tattersall, 2003; Bae, 2010). This partial cranium (Figs. 1 and 2) was found in the cave sediments of a deep, narrow, and dark crevice, and its original stratigraphic section cannot be established with certainty. According to the associated faunal remains, Maba was tentatively assigned to the Middle Pleistocene (Liang and Li, 1959), the Middle-Late Pleistocene transition (Guangdong Museum, 1959; Woo and Peng, 1959), and Late Pleistocene (Xu and Huang, 1988). Maba 1 chronology possibly ranges between 135 and 129 ka (MIS 5e) according to a vertebrate teeth dating based on uranium methods (Yuan et al., 1986). A $^{30}Th/^{234}U$ dating of capping flowstone samples from a South Branch Cave suggests that the Maba 1 cranium possibly dates to the late Middle Pleistocene (MIS 7–6) (Gao et al., 2007). Recently, Shen et al. (2014) presented a new mass-spectrometric U-series dates based on speleothem samples intercalated with deposits in Southern Branch Cave, and suggested that Maba hominid should thus be at least 230 ± 5 ka old, most probably older than 278 ± 4 ka. Given that the South Branch Cave is over 30 meters away from the crevice where Maba cranium was found, the date remains problematic. Because of the dating range from Middle Pleistocene to Late Pleistocene, and taking into account the limits in associating specific geochronological references with the human remains, any evolutionary interpretations must necessary deal with a large chronological uncertainty (Xiao et al., 2014)

After the reconstruction of the skull performed by Wu Rukang in 1959, most authors recognized traits resembling both archaic Asian specimens (i.e., Zhoukoudian *Homo erectus*) and Neandertals, in this latter case mostly because of its facial morphology (see Woo and Peng, 1959; Wu, 1988; Pope, 1992). As in Neandertals, the upper face of Maba is characterized by a thick and circular profile of the orbit, and a narrow, pinched, and projecting nasal bone. Figure 3 show a visual comparison between Maba 1 and Saccopastore 1, a European specimen dated at the transition between Middle and Upper Plesitocene (Bruner and Manzi, 2006). However, only a minor portion of the face is available for Maba 1,

Grant sponsor: External Cooperation Program of BIC, Chinese Academy of Sciences; Grant number: GJHZ201314; Grant sponsor: Spanish Government (to E.B.); Grant number: CGL2012-38434-C03-02; Grant sponsor: Italian Institute of Anthropology; Grant sponsor: National Natural Science Foundation of China (to X.W.); Grant number: 41272034; Grant sponsor: Chinese Academy of Sciences; Grant number: KZZD-EW-03.

*Correspondence to: E. Bruner; E-mail: emiliano.bruner@cenieh.es

Received 27 October 2015; revised 1 February 2016; accepted 18 February 2016

DOI: 10.1002/ajpa.22974
Published online 00 Month 2016 in Wiley Online Library (wileyonlinelibrary.com).

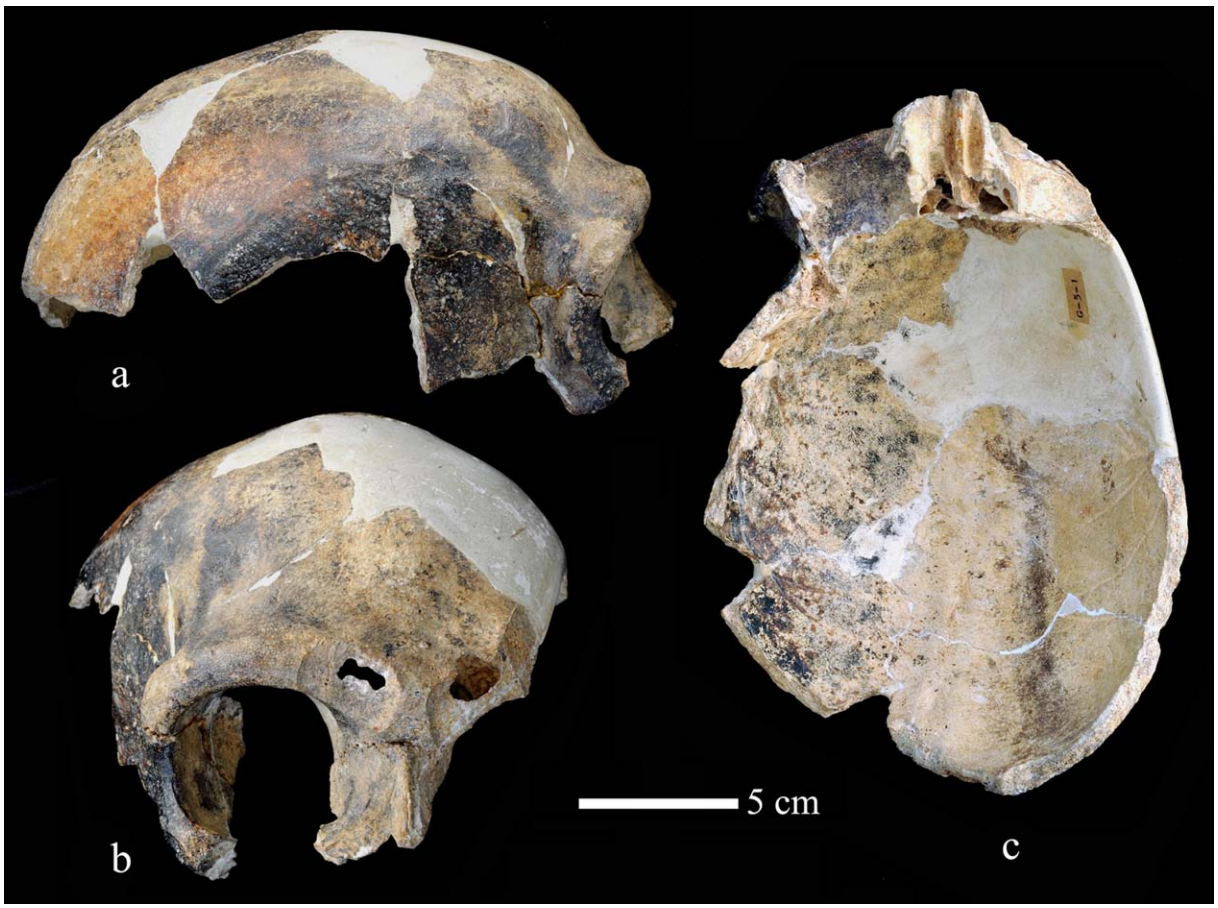

Fig. 1. Maba 1, in right lateral (a), frontal (b), and inferior (c) views. The areas reconstructed with plaster in 1959 are visible in white.

and a proper evaluation of its supposed Neandertal features is still missing. Other characters which deserve attention in the Maba skull include the vertical frontal squama, the frontal keel and the thin vault (Woo and Peng, 1959; Bräuer and Mbua, 1992). Because of this combination of traits, Maba 1 was generally considered to represent an archaic taxon which is somehow intermediate between small-brained and large-brained human species.

In this study, we present a quantitative analysis of the endocast of Maba 1, providing a description of its endocranial features, and metric comparisons to evaluate its endocranial proportions within the variation of the human genus. Beyond any difference in cranial capacity, large-brained human taxa—namely modern humans and Neandertals—display specific changes in their endocranial traits and geometry (Bruner et al., 2003; Bruner, 2004; Gunz et al., 2010), while archaic humans—namely *H. ergaster*, *H. erectus*, and *H. heildelbergensis*—share a similar endocranial appearance (Bruner et al., 2015). This study is therefore aimed at evaluating whether Maba 1 displays a derived phenotype of the braincase, or if it retains a plesiomorphic endocranial organization.

MATERIALS AND METHODS

The fragments from Maba 1 were assembled back in 1959 by using plaster, most of all to reconstruct parts of the left frontal areas (Fig. 2). Segments of the right coronal, sagittal, and lambdoid sutures are visible on the cranium, and the position of bregma and lambda can be then extrapolated and are accurately marked. Therefore, the relative position of the frontal and parietal bones can be inferred with a little uncertainty. The neurocranium of Maba 1 is only represented by its frontal and parietal areas, and a little portion of the temporal pole. Although the braincase is incomplete, the frontal and parietal districts are informative in terms of paleoneurology, because of their morphological correspondence with the underlying brain form, which include cortical areas relevant for human evolution.

The skull was CT scanned at the Institute of Vertebrate Paleontology and Paleoanthropology, Chinese Academy of Sciences (IVPP), in coronal orientation through a high-resolution industrial CT scanner (450 kV-ICT), at 430 kV 9 mA, pixel matrix 1024 × 1024, and 0.3 mm voxel size. Imaging was performed with MIMICS 16.0 (Materialise, Belgium), reconstructing the digital replicas of the skull and endocast (Figs. 4 and 5). Zhoukoudian V (Wu et al., 2010a) was used as reference to perform a 3D reconstruction of the endocast. The current morphometric study, however, only concerns the original endocranial areas, and the digital reconstruction must be considered as an aid to help visualization only.

A total of 96 endocasts which represent *H. erectus* ($n = 21$), Afro-European Middle Pleistocene ($n = 6$), Neandertals ($n = 13$), early modern humans ($n = 6$), and recent modern humans ($n = 50$) were used as morphometric comparative sample (Tables 1 and 2). Specimens were sampled

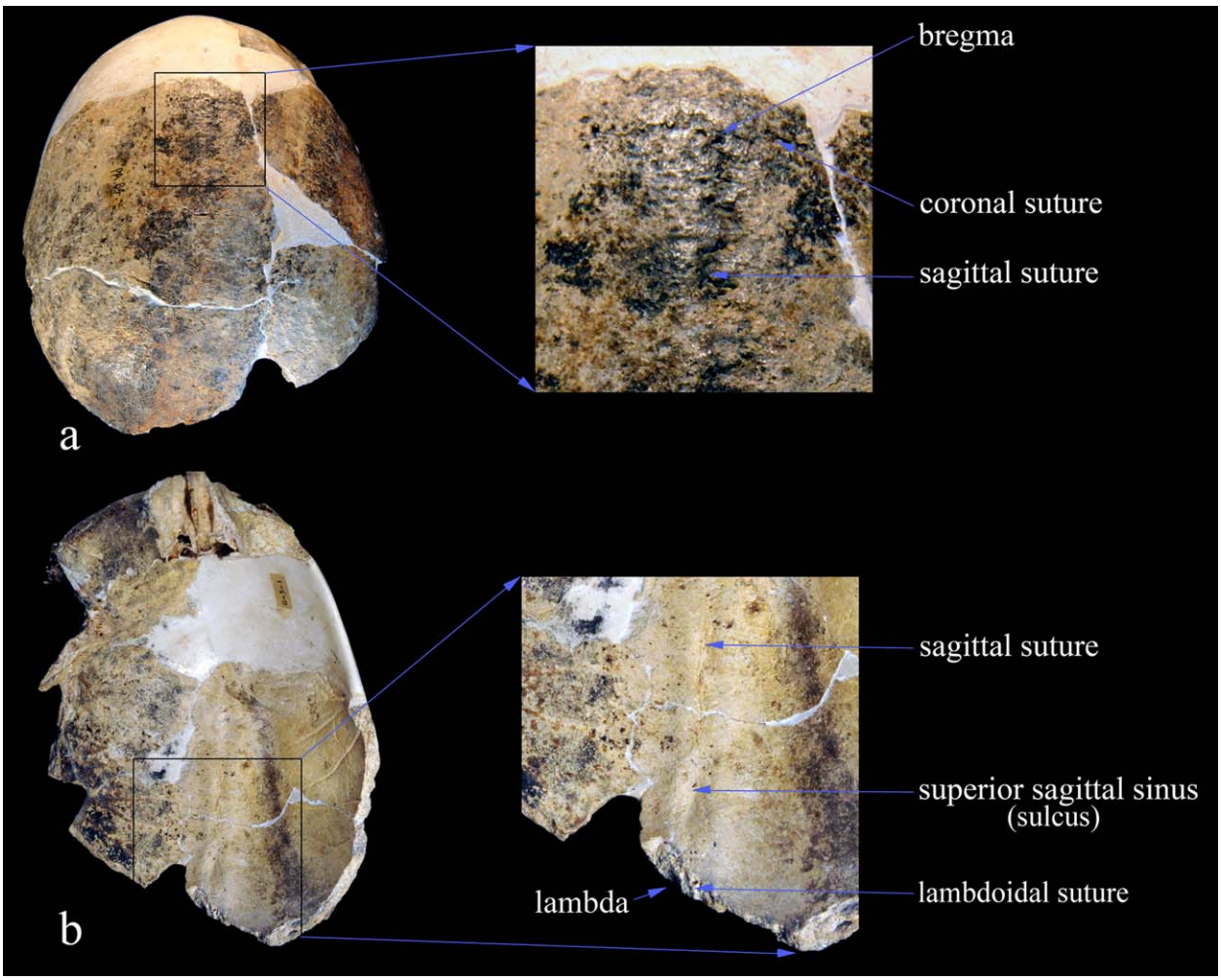

Fig. 2. The superior (a) and endocranial view (b) of Maba 1, showing the position of bregma, coronal suture, sagittal suture, the sulcus of the superior sagittal sinus, lambdoidal suture, and lambda.

at the IVPP (Beijing) and from the Ralph Holloway endocast collection (Columbia University, New York). Data on Minatogawa 1 and Saccopastore 1 are available from published literature (Kubo et al., 2008; Bruner and Manzi, 2008).

Endocranial arcs and chords were measured to compare and quantify the endocranial form of Maba 1 (Fig. 6). Taking into account the available anatomical information, only nine variables can be measured on the Maba endocast: parietal chord length (PCOR), parietal arc length (PARC), maximum width chord (MWC), maximum Broca width (MBW), maximum frontal width (MFW), frontal height (FH), superior cerebral height (SCH), frontal chord length (FCOR) and frontal arc length (FARC). SCH was measured estimating the antero-posterior (fronto-occipital) orientation, according to the reconstruction of the endocast. All measures were sampled by the same observer (XW). Each endocast was measured three times, and the average value for each variable was used as final measurement. The ratio between the Broca's width and the maximum width was used to quantify the degree of frontal narrowing. The ratio between arc and chord for the frontal and parietal bone were used to quantify the degree of frontal and parietal bulging, respectively.

UPGMA clustering was used to compare fossil specimens by using their raw values. This clustering procedure is aimed at quantifying the overall resemblance and phenotypic affinity between the specimens, and not to evaluate the statistical coherency of the groups. The multivariate structure of the sample was analyzed by means of Principal Component Analysis (PCA). PCA was computed with frontal and parietal arcs but excluding frontal and parietal chords, to avoid data redundancy and to reduce the effect of multicollinearity (Jolliffe, 2002). The results do not show any relevant change when adding the chords to the analysis, and the study of the relationships between chords and arcs will be hence limited to their ratios. PCA was computed on the correlation matrix, as to standardize the intra-group variation. However, using the covariance matrix (and therefore considering the absolute values) the analysis gave similar results. Because of the small sample size for each group and the incompleteness of the specimens, inferential statistics (like discriminant analysis or canonical variates analysis) is not sufficiently reliable, and the current numerical analyses must be intended as a quantification of the observed differences between specimens and within the sample.

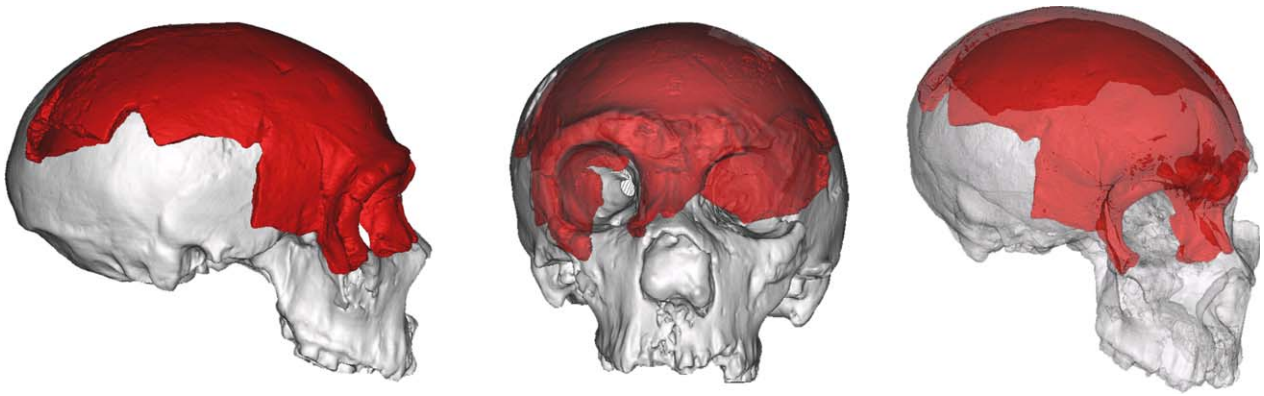

Fig. 3. Maba 1 was hypothesized to show a facial morphology resembling Neandertals. In this image, Maba 1 (red) is superimposed on Saccopastore 1 (white), a European early Neandertal dated to the transition between Middle and Upper Plesitocene.

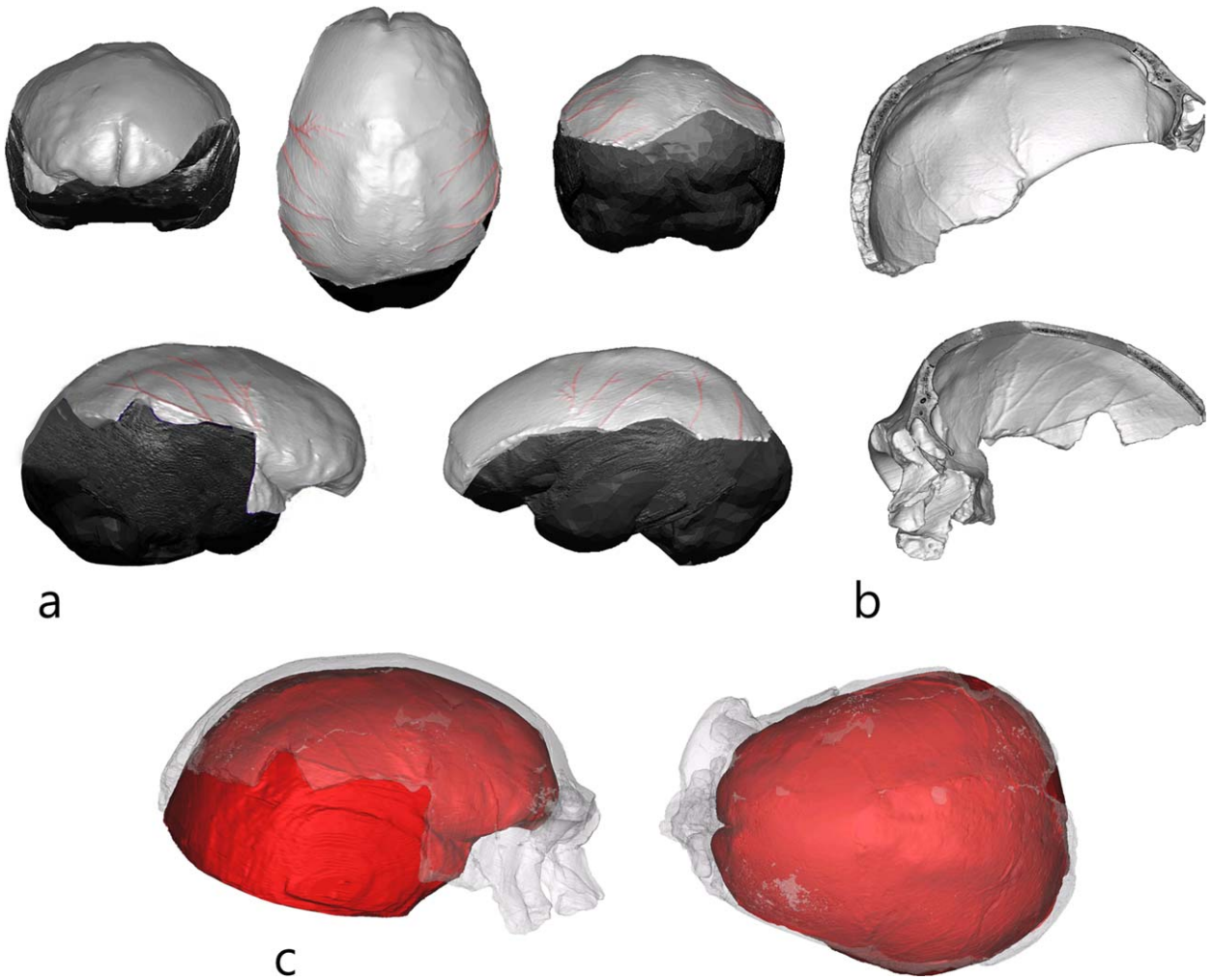

Fig. 4. (a) the Maba 1 endocast, showing its frontoparietal morphology and the course of the middle meningeal vessels (the endocast of Zhoukoudian V was used to complete partially the missing areas for visualization purposes—dark gray surface), (b) The endocranial surface is rendered and oriented in order to show the traces of the middle meningeal vessels, (c) the endocast reconstruction viewed together with the transparent digital replica of the skull.

The cranial capacity of Maba 1 was estimated by using multiple regression between cranial capacity and the metric variables for the rest of the sample (whole sample and fossils only). We also used the first principal component as a size-related vector, establishing a regression between this vector and the cranial capacity of the rest

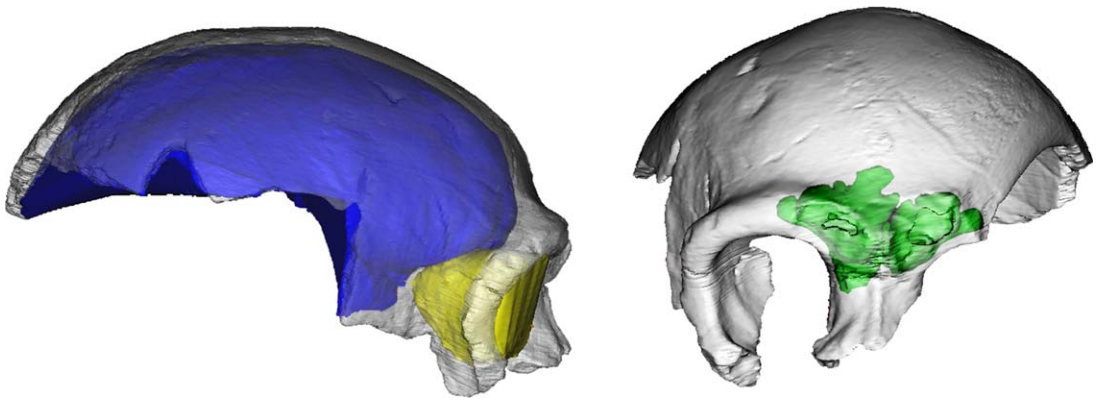

Fig. 5. In lateral view (left), it can be seen that the anterior part of the endocranial cavity (in blue) stands above the orbits (in yellow). As can be seen in the frontal view (right), the frontal sinuses (in green) are modest but well developed, reaching almost half of the browridge.

TABLE 1. Comparative sample (n = 96)

H. erectus (HE, $n = 21$)	Zhoukoudian (ZKD) 2, 3, 5, 10, 11, 12, Hexian 1 (HEX), Nanjing 1 (NAJ), Trinil 2 (TN2), Sangiran 2,17 (SNG), Sambungmacan 3 (SBM3), KNM-WT15000 (WT15000), Salé (SAL), KNM 3733, KNM 3883, Ngandong 1, 6, 7, 12, 14 (NG)
African/European Middle Pleistocene *Homo* (MPL, $n = 6$)	Arago XLVII (ARG), Kabwe (KBW), Bodo, Swanscombe (SWC), Jebel Irhoud I (JE1), Laetoli 18 (LL18),
Neandertals (NDR, $n = 13$)	La Chapelle-aux-Saints (CHP), La Ferrassie 1 (FRS), La Quina 5 (LQN), Spy 1 and 2, Feldhofer Neandertal l (NDR), Monte Circeo Guattari 1 (GTT), Amud 1 (AMD), Krapina 3 and 6 (KRP), Reilingen (REL), Gibraltar 1 (GBR), Saccopastore 1 (SCP1)
Early modern humans (EMH, $n = 6$)	Predmost 3, 4, 9, 10 (PRD), Liujiang 1(LJ), Minatogawa I (MW)
Recent humans (MOD, $n = 50$)	Worldwide

TABLE 2. Metric variables and definitions

Measurement	Description
PCOR	Parietal chord length: the Euclidean distance between the endobregma and the endolambda
PARC	Parietal arc length: the arc distance between the endobregma and the endolambda
MWC	Maximum width: the maximum width of the endocasts
MBW	Broca width: the endocranial width at the Broca's caps
MFW	Frontal width, the endocranial width at the coronal eminence
FH	Frontal height: the distance from the endobregma to the bottom of the frontal cap, as projected on the midsagittal plane
SCH	Superior cerebral height: the vertical length from the fronto-occipital plane to the top of the endocast
FCOR	Frontal chord length: the Euclidean distance from the frontal pole to the endobregma, as projected on the midsagittal plane
FARC	Frontal arc length, the arc distance from the frontal pole to the internal bregma, projected on the midsagittal plane

of the sample. A size-related principal component, as a linear combination based on the within sample correlations, can be less sensitive to noise introduced by individual values or variables, when compared with multiple regression. Regression parameters were then used to estimate the Maba cranial capacity. Statistics was performed with PAST 2.12 (Hammer et al., 2001) and Statistica 12 (Statsoft).

RESULTS

The CT scan and reconstructed endocast provide evidence of both primitive and derived features of Maba 1. The Maba 1 endocast preserves a large part of the frontal and parietal areas, as well as a minor part of the right temporal pole (Figs. 4 and 5). The left temporal, occipital, and cerebellar areas are missing. The frontal lobes are narrow when compared with the endocranial width, with the left pole protruding relative to the right one. The sulcal pattern is visible on the right side. The parietal areas show a clear parasagittal depression, although the midline does not present a continuous central keeling. The traces of the middle meningeal vessels of the upper vault are visible, suggesting the dominance of the anterior branches and, although the network is composed of many channels, absence of anastomoses. The frontal lobes lie on the orbital roof, and the frontal sinuses show a moderate development reaching almost half of the upper orbit outline, and the base of the frontal squama.

According to the ratios available for this specimen (Fig. 7), the frontal lobes of Maba 1 are very narrow but display a marked anterior bulging of the sagittal profile.

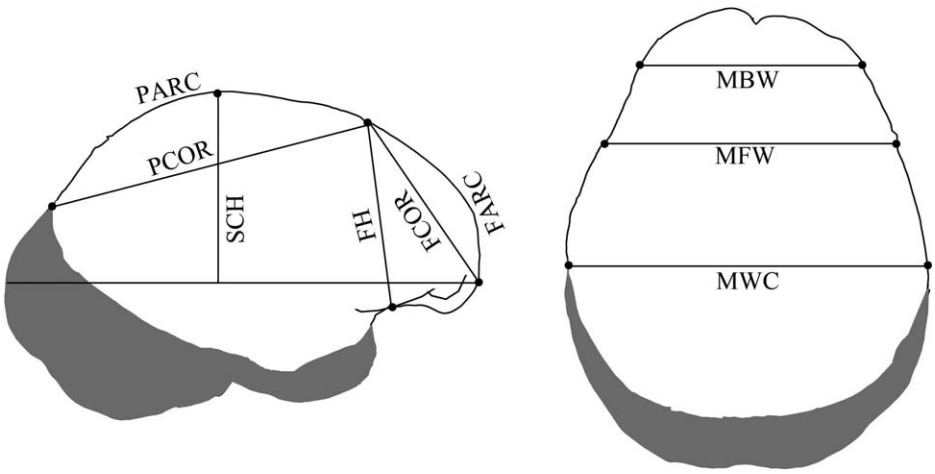

Fig. 6. In this morphometric analysis, only the available diameters were used to compare Maba 1 with the rest of the sample. The only extrapolated reference was the fronto-occipital axis, used to estimate the maximum vault height. The frontal parietal chords were used only to calculate the frontal and parietal bulging, and were not used in the multivariate analyses.

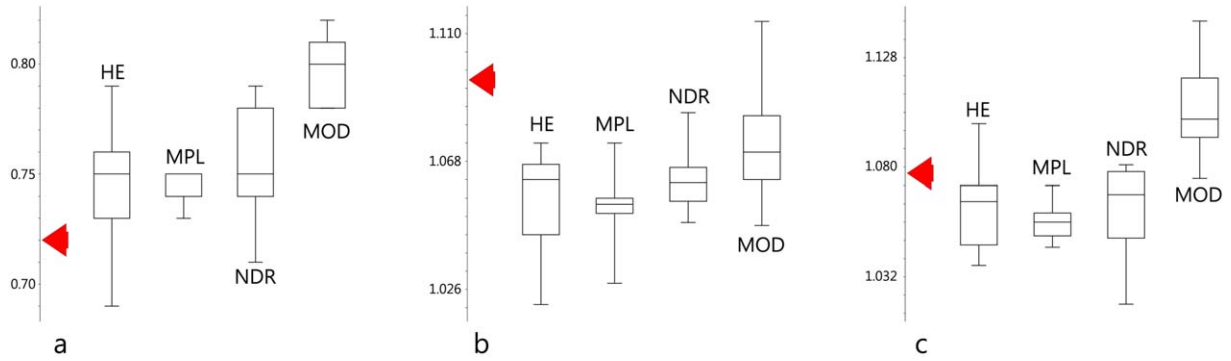

Fig. 7. The boxplots show the distribution (median, interquartile and range, three outliers excluded) for *Homo erectus* (HE), Afro-European Middle Pleistocene (MPL), Neandertals (NDR) and modern humans (MOD), for frontal widening at the Broca's cap (a: MBW/MWC), frontal bulging (b: FARC/FCOR), and parietal bulging (c: PARC/PCOR). The value of Maba 1 is evidenced with the arrow.

The parietal profile is not bulging, and its curvature is comparable with any nonmodern human taxon.

Taking into account, all the measures together and computing a UPGMA analysis, Maba 1 clusters with Kabwe and Reilingen (Fig. 8). The cophenetic correlation coefficient of this phenogram is modest ($R = 0.72$) suggesting that, although the clusters may show general phenotypic affinities, groups are not stable and possibly sensitive to individual components. The first branching separating a cluster of *H. erectus* from the rest of the sample is supported 100% when variables are bootstrapped, but the rest of the branches do not reach 50%. When the whole modern human sample is included in the analysis, the cluster formed by Kabwe, Reilingen, and Maba, is confirmed. When the analysis is computed on sample normalized data (z scores), Maba clusters with Bodo, Zhoukoudian 10, and Ngandong 1.

PCA shows a morphological space characterized by only one dominant component, which explains 72% of the variance (Fig. 9). The second component explains 12% of the variance. This second vector is above the Jolliffe threshold value, but not above the broken stick model of random variation. Hence, its stability must be considered with caution. The following components explain less than 6% of the variance and are below any conventional threshold of reliability, and they will not be considered here. PC1 is a size-related vector, associated with a relative increase of all the variables. PC2 is associated with an increase of parietal length and height, and decrease of width. The same morphological components have been obtained by using other endocranial data (Bruner et al., 2003). Therefore, despite the limited stability of the second axis, this multivariate space is consistent with the current information on the endocranial variability of the human genus. According to this multivariate space, *H. erectus* and Neandertals are mainly separated by increased size and widths in the latter group, and modern humans are separated by nonmodern humans by means of their larger parietal diameters. Within this space, Maba 1 is positioned in an overlapping morphological area among Neandertals, Afro-European Middle Pleistocene, and modern humans. This result suggests that the overall neurocranial proportions of Maba 1 are not able to reveal any species-specific morphological affinity. Interestingly, the Afro-European Middle Plesitocene group is widely scattered throughout this PC space: Arago within the *Homo erectus* range, Swanscombe,

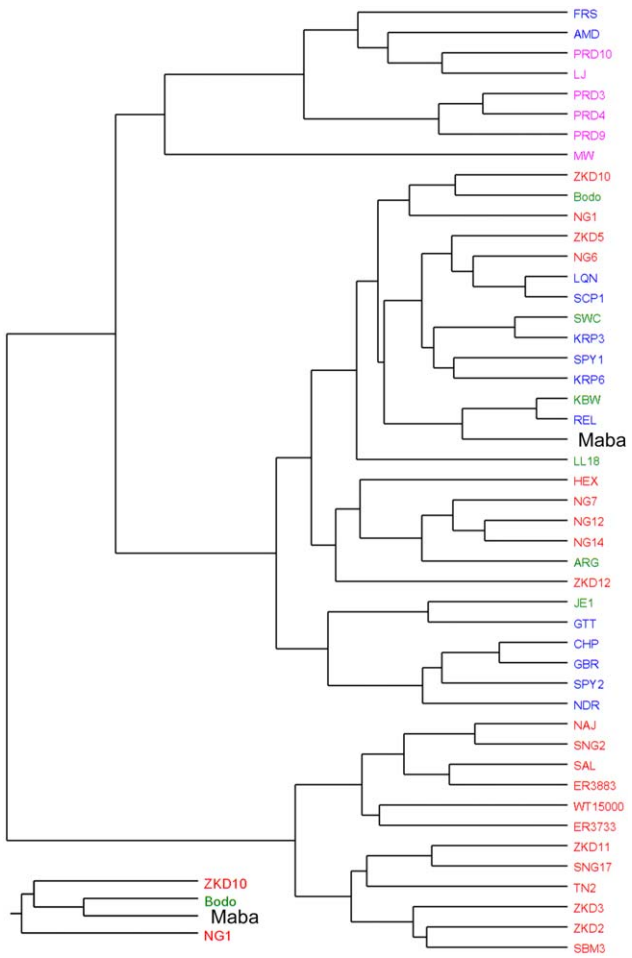

Fig. 8. UPGMA clustering showing the morphological similarities among the fossil specimens of the sample (red: *Homo erectus*; blue: Neandertals; green: Afro-European Middle Pleistocene; purple: *Homo sapiens*; see Table 1 for labels). Below, the cluster including Maba when using normalized values (*z* scores).

Kabwe and Jebel Irhoud within the Neandertal range, Laetoli 18, and Bodo within the modern human range. Within this multivariate space, Zhoukoudian 10 is the *H. erectus* which is closest to Maba, and Saccopastore 1 the closest Neandertal.

A multiple regression between cranial capacity and the metric variables provide an estimation of the Maba cranial capacity of 1296 cc (all sample; $R^2_{adj} = 0.93$; 95% CI 1243–1349 cc), and 1291 cc (fossil sample; $R^2_{adj} = 0.94$; 95% CI 1182–1400 cc). PC1 is also an efficient and synthetic size-related vector, which is strongly correlated with cranial capacity, for the whole sample ($R = 0.95$; $P < 0.0001$) or for the fossil sample only ($R = 0.96$; $P < 0.0001$). Using a least-square regression between PC1 (independent variable) and cranial capacity (dependent variable), and using the residuals between observed and expected values for each specimen to calculate the standard deviation of the uncertainty, the cranial capacity estimation for Maba 1 is 1331 ± 75 cc and 1342 ± 79 cc, when using the whole sample or only the fossil specimens, respectively.

A further PCA was computed on values adjusted for each specimen according to their individual geometric mean, as to evaluate their individual proportions. In this case, there are two significant principal components, separating *H. sapiens* (relatively taller braincase) from the rest of the sample (relatively wider braincase). Namely, this adjustment eliminates the differences between *H. erectus* and Neandertals. The two resulting groups, modern and nonmodern humans, display however a moderate overlap, and Maba is positioned right in the center of this shared morphological zone, as in the previous analysis (data not shown).

DISCUSSION

The endocranial morphology of Maba 1

The estimated cranial capacity of Maba, around 1300 cc, is within the normal range of modern humans and Neandertals, and slightly above the *H. heidelbergensis* average figure, which is around 1200 cc (Rightmire, 2004). It must be cautiously considered that, at least for modern humans for which we have statistical data, brain size can commonly show a degree of variation spanning 400–700 cc (Holloway, 1980; Allen et al., 2002), and ranging from 900 to 2000 cc (Holloway et al., 2004). Therefore, stringent conclusions based on any minor difference of cranial capacity, like those among these human species or even among specimens, should be avoided. Accordingly, we can only conclude that the cranial capacity of Maba 1 is compatible with most Middle-Upper Pleistocene hominid species. Also when considering the general endocranial proportions through a multivariate analysis, Maba is positioned at a crossing point among *H. heidelbergensis*, Neandertals, and modern humans.

The anterior fossa of Maba 1 shows archaic proportions but derived spatial relationships with the facial block. The frontal lobes are narrow when compared with the general endocranial width. Such narrow frontal lobes are the endocranial counterpart of the marked postorbital constriction, which has been already evidenced in this specimen (Pope, 1992). Although there is a great intra-specific variation associated with this trait, the proportions of Maba 1 are generally displayed by archaic taxa like *H. erectus* and *H. heidelbergensis*, while Neandertals and modern humans display relatively wider frontal areas (Bruner and Holloway, 2010).

Despite the narrow prefrontal cortex, the frontal squama of Maba 1 is nonetheless curved and bulging sagittally, as in *H. sapiens*. A shape analysis of its outer profile confirmed its modern appearance, evidencing a similarity with Jebel Irhoud or with the Qafzeh/Skhul specimens (Bruner et al., 2013). Nonetheless, the same study also showed overlapping between the variation of modern and nonmodern humans, suggesting caution when considering this trait alone. The bulging of the frontal squama is often scored in modern humans as a female trait, but it should be evaluated whether or not this difference can be also found in extinct hominids. As a matter of fact, this character shows chronological and geographical differences even within the variation of *Homo erectus* (Antón, 2003). However, apart from their archaic general proportions, the frontal lobes are positioned right on the orbital roof, as in Neandertals and modern humans (Bruner and Manzi, 2008). In all archaic human forms, the frontal lobes are in a more posterior position relative to the facial block (Bookstein et al., 1999; Bruner and Manzi, 2005). Moreover, in Maba 1 the size of the frontal sinuses is larger when compared with other Asian specimens (Pope, 1992).

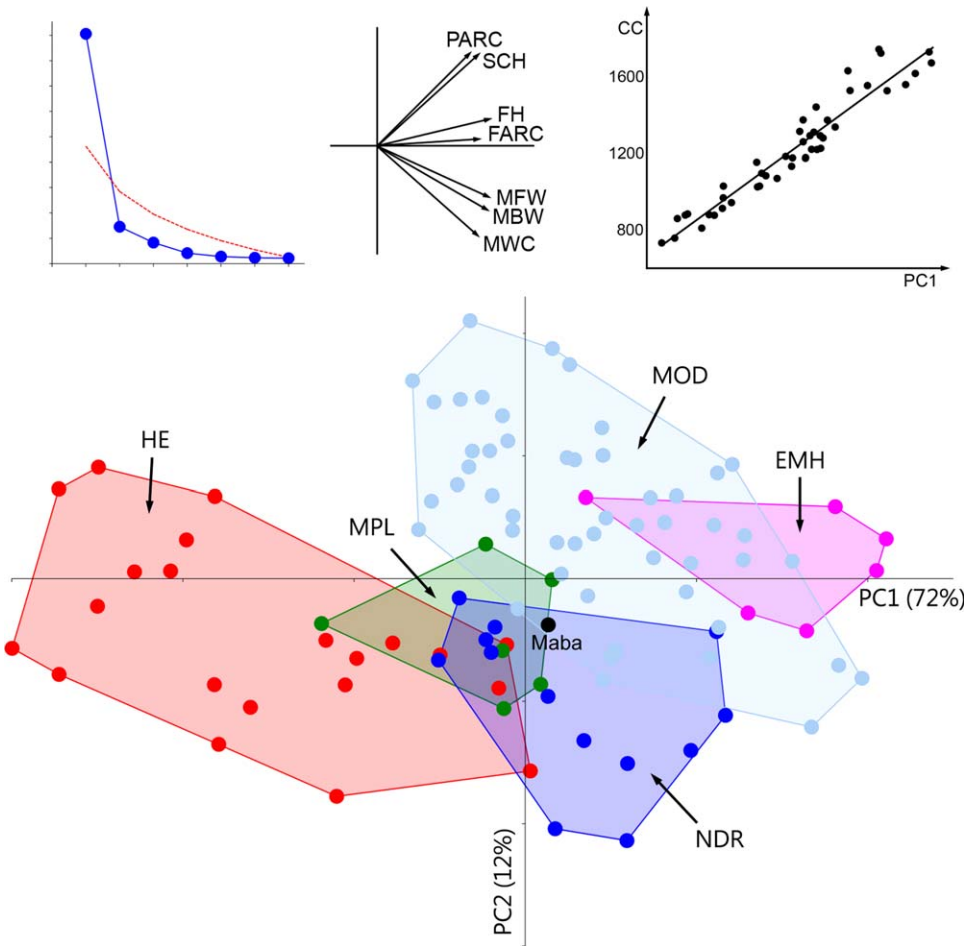

Fig. 9. Principal component analysis. Above: scree plot and broken stick level (left), vector distribution of the variables along the two principal components (middle), and correlation between PC1 and cranial capacity (CC) for the fossil sample (right). Below: distribution of the groups according to the first two principal components. PC1 is a size vector. PC2 separates *Homo sapiens* according to the large parietal arc and vault height.

Their morphology is comparable with the patterns described for modern humans and Neandertals (Bruner and Manzi, 2008; Zollikofer et al., 2008), but different from *H. heidelbergensis*, in which the frontal sinuses expand much more into the frontal squama (Seidler et al., 1997; Prossinger, 2008).

In sum, Maba 1 shows a plesiomorph condition for its frontal lobe proportions (relative width), but a derived condition when considering the structural organization between brain and face, namely the spatial relationship between frontal lobes and orbits, the morphology of the frontal sinuses, and possibly the curvature of the frontal squama.

Parietal endocranial morphology of Maba 1 does not present any derived trait. The parietal areas do not show the midsagittal bulging displayed by modern humans (Bruner et al., 2011). Maba 1 does not even display the upper lateral bulging characterizing the Neandertals parietal areas, and its upper parietal surface is depressed parasagittally, as in *H. erectus* (Grimaud-Hervé, 1997; Bruner et al., 2015) and *H. heidelbergensis* (Bruner et al., 2003). The vascular pattern associated with the endocranial surface of Maba 1, although showing several branches, does not display a complex network as in modern humans.

The vascular system is not particularly developed in the posterior endocranial districts as in many Asian *H. erectus* specimens, and the pattern is comparable with *H. heidelbergensis* and Neandertals (Grimaud-Hervé, 1997; Bruner et al., 2005; Wu et al., 2010b). Therefore, we can conclude that the morphology of the parietal area in Maba 1 is essentially plesiomorphic, without evidence of derived traits.

Taking into account cranial capacity and the archaic endocranial characters, it is hence not surprising that the Maba 1 braincase shows proportions compatible with the overlapping ranges among Middle Pleistocene and Upper Pleistocene taxa, being morphologically similar to specimens which are generally included in the hypodigm of *H. heidelbergensis* like Kabwe and Bodo, or intermediate between *H. heidelbergensis* and *H. neanderthalensis* like Reilingen (Dean et al., 1998). It must be taken in mind that, at present, observed endocranial differences between *H. erectus* and *H. heidelbergensis* are only a matter of size, and no morphological traits are able to separate these two taxa. Therefore, the endocranial morphology of Maba 1 must be interpreted as generally archaic, with a brain size that approaches this specimen to *H. heildelbergensis*.

Maba 1 and the evolution of the human genus

Morphology, mostly when based on small samples or individual specimens, is often not a sufficient source of phylogenetic information (e.g., Tattersall, 1986; Albrecht and Miller, 1993; Plavcan and Cope, 2001; Bruner, 2013). Taking into consideration the wide geographical and chronological range of Middle Pleistocene hominid species, the large phenotypic variation, and the lack of strict correspondence between morphology and taxonomy, firm phylogenetic conclusions on single specimens are largely speculative. Within the human genus, many traits show overlapping ranges of variation in different species, and they can be often the expression of individual features. Taking into account that intraspecific variation can be large and inter-specific differences can be subtle, large samples are necessary to provide robust statistical inferences able to detect significant dissimilarity. In many paleoanthropological cases, the scarce fossil record hampers a consistent quantitative approach, and this limit is apparent for the Asian fossil record because of its dispersed chronological and geographical range (Bruner et al., 2015).

All these limits are further patent when dealing with the human diversity associated with Middle Pleistocene. In the last decades several specimens have been grouped into *H. heidelbergensis*, a taxon with derived features when compared with *H. ergaster*/*erectus* (Rightmire, 1998). The limited anatomical information and large geographical and chronological range hampered a general agreement on the taxonomic and phylogenetic interpretation of this species. A main issue concerned whether or not the European and African populations belong to the same phylogenetic process (Rightmire, 2008). Lately, also the homogeneity within the European samples was questioned (Stringer, 2012). In all cases, the Asian record was largely missing, and this represents a major limit to every demographic and phylogenetic hypothesis on human evolution in Middle Pleistocene. Despite the difficulties in defining clear boundaries for this species, it can be still characterized according to a set of anatomical features (Mounier et al., 2009), and a crucial role of East Asia for the evolution and dispersal of *H. heidelbergensis* cannot be, at present, excluded (Buck and Stringer, 2014).

The endocast of Maba shows a plesiomorphic appearance, comparable with a general archaic phenotype with narrow frontal lobes, flattened parietal surface, and simple vascular patterns. The only character which can be possibly interpreted as derived is the spatial relationships between brain and face, because of the position of the prefrontal cortex, curvature of the frontal squama, and size of the frontal sinuses. Interestingly, the upper facial morphology of Maba was supposed to show a general resemblance with the Neandertal phenotype. The mosaic morphology of Maba 1 cranium, with Neandertal-like facial traits and plesiomorph (*H. heidelbergensis*) neurocranial phenotype, is hence reminiscent of European specimens like Sima de los Huesos (Arsuaga et al., 2014). In Europe, during the Middle Pleistocene, it has been hypothesized that Neandertal traits were first recognized in the facial block, and later on the neurocranial areas, with a general evolutionary trend proceeding from the anterior to the posterior districts of the skull. As in Maba, in the sample from Sima de los Huesos Neandertal characters of the face are associated with more archaic endocranial morphology (Bruner et al., 2003). Saccopastore 1, which is dated approximately to the transition between Middle and Upper Pleistocene, displays an upper facial morphology similar to Maba 1 but a more typical Neandertal endocranial form (Bruner and Manzi, 2008). In Europe, an *accretion model* was proposed to interpret the progressive appearance of Neandertal features (Dean et al., 1998), but bottlenecks and other more discontinuous changes cannot be ruled out (Bruner and Manzi, 2006). Overall, the fossil record does not allow a complete evaluation of the chronological and geographical patterns behind the human transition in Europe from Middle to Late Pleistocene, and there is no agreement on the mechanisms underlying the observed morphological changes (see e.g., Hawkes and Wolpoff, 2004; Hublin, 2009 for contrasting perspectives). If Maba 1 is associated with the Neandertal lineage, its phylogenetic position may be similar to the sample from Sima de los Huesos: Neandertal facial traits with a plesiomorphic braincase. Independently of whether or not this process was anagenetic or characterized by successive isolations and more discrete changes, in this case we would deal with a widespread Euro-Asian paleospecies. Demographic relationships between Europe and Asia has been hypothesized on the large (Xing et al., 2015) and short (Wu, 2004) chronological scale. Other Chinese specimens have been described as showing morphological features affine to the Neandertal phenotype (Wu et al., 2014; Wu and Trinkaus, 2014; Xing et al., 2015). Neandertal presence has been confirmed in central Asia and Siberia by genetic analyses, and this may suggest that their territories could have reached also the eastern areas of the continent (Krause et al., 2007; Prüfer et al., 2014). However, only the upper facial morphology is available for Maba 1, and a detailed phylogenetic analysis of its traits is still missing. Therefore, this general facial resemblance must be properly evaluated yet.

As alternative hypothesis, the morphology of Maba can be the result of convergence and multiple migration patterns, and part of an evolutionary history which is independent of the European lineages. Many Asian fossils dated to the transition between Middle and Late Pleistocene are not easily accommodated within the Afro-European fossil taxa, suggesting complex evolutionary patterns involving processes of immigration or even admixture (Pope, 1992; Bae, 2010). Furthermore, because of the shared structural and functional organization among closely related taxa, hominid evolution is sensitive to parallelism and convergences (Collard and Wood, 2000). The fronto-parietal morphology of the human genus suggests in fact that the migration patterns were not simply based on linear pulses or simple dynamics (Gunz et al., 2009). In this case, Maba 1 should be interpreted as an archaic Chinese hominid, and any resemblance with Neandertals would be the result of a wide variation, homoplasy, and idiosyncratic characters, without any clear phylogenetic signal. Actually, the recent genetic studies on Siberian Late Pleistocene samples suggest the possibility that Asia had a population history partially distinct and independent from Neandertals in Europe, with groups which morphology and appearance is, to date, not known (Reich et al., 2010; Sawyer et al., 2015). In this case it remains to be established whether Maba 1 could have belonged to populations before or after such hypothetical branching event between the two geographic areas.

Interestingly, at the transition between Middle and Late Pleistocene, we can find in Asia individuals like Maba with "Neandertal face" and "archaic braincase", and in Africa individuals like Jebel Irhoud, with "modern face" and "Neandertal braincase" (Bruner and Pearson, 2013). Currently, no evolutionary hypothesis is still able to accommodate comfortably such scattered and heterogeneous variability, beyond a level of general perspectives. Increasing the sample is hence the mandatory step to enhance and test comprehensive evolutionary theories. Certainly, we must be aware that different chronological periods and distant geographical areas may have undergone distinct evolutionary mechanisms, and search for one single shared process may be misleading.

CONCLUSIONS

The chronology of Maba 1 is tentative, and the fossil can be approximately dated to the end of the Middle Pleistocene, although with a large range of uncertainty. Its cranial morphology combines upper facial features affine to Neandertals with a more archaic braincase. If this is the result of demographic and genetic variation shared with the European Middle Pleistocene human groups, it provides a further piece of an intercontinental evolutionary process, and it suggests a revision of the biogeographic ranges associated with the Neandertal lineage. The endocranial anatomy appears to lack any evidence of derived features able to support more complete phylogenetic perspectives. A detailed analysis of its facial traits is therefore necessary to evaluate any further taxonomic inference.

ACKNOWLEDGMENTS

We thank Aida Gómez-Robles and two referees for their comments on an early version of the article. We are extremely grateful to Ralph Holloway for his constant support, and for the passion and commitment he devoted to paleoneurology throughout the years.

LITERATURE CITED

Albrecht GH, Miller JMA. 1993. Geographic variations in Primates: a review with implications for interpreting fossils. In: Kimbel WH, Martin LB, editors. Species, species concepts, and primate evolution. New York: Plenum Press. p 123–162.

Allen JS, Damasio H, Grabowsky TJ. 2002. Normal neuroanatomical variation in the human brain: an MRI-volumetric study. Am J Phys Anthropol 118:341–358.

Antón S. 2003. Natural history of Homo erectus. Yearb Phys Anthropol 46:126–170.

Arsuaga JL, Martinez I, Arnold LJ, Aranburu A, Gracia-Tellez A, Sharp WD, Quam RM, Falgueres C, Pantoja-Perez A, Bischoff J, Poza-Rey E, Pares JM, Carretero JM, Demuro M, Lorenzo C, Sala N, Martinon-Torres M, Garcia N, de Velasco A. 2014. Neandertal roots: cranial and chronological evidence from Sima de los Huesos. Science 344:1358–1363.

Bae CJ. 2010. The Late Middle Pleistocene hominin fossil record of Eastern Asia: synthesis and review. Yearb Phys Anthropol 53:75–93.

Bookstein F, Schäfer K, Prossinger H, Seidler H, Fieder M, Stringer C, Weber GW, Arsuaga JL, Slice DE, Rohlf FJ, Recheis W, Mariam AJ, Marcus LF. 1999. Comparing frontal cranial profiles in archaic and modern *Homo* by morphometric analysis. Anat Rec 257:217–224.

Braüer G, Mbua E. 1992. *Homo erectus* features used in cladistics and their variability in Asian and African hominids. J Hum E 22:79–108.

Bruner E. 2004. Geometric morphometrics and paleoneurology: brain shape evolution in the genus *Homo*. J Hum E 47:279–303.

Bruner E. 2013. The species concept as a cognitive tool for biological anthropology. Am J Primatol 75:10–15.

Bruner E, Athreya S, Manuel de la Cuétara J, Marks T. 2013. Geometric variation of the frontal squama in the genus *Homo*: frontal bulging and the origin of modern human morphology. Am J Phys Anthropol 150:313–323.

Bruner E, De la Cuétara JM, Holloway R. 2011. A bivariate approach to the variation of the parietal curvature in the genus *Homo*. Anat Rec 294:1548–1556.

Bruner E, Holloway R. 2010. Bivariate approach to the widening of the frontal lobes in the genus *Homo*. J Hum E 58:138–146.

Bruner E, Manzi G. 2005. CT-based description and phyletic evaluation of the archaic human calvarium from Ceprano, Italy. Anat Rec 285A:643–658.

Bruner E, Manzi G. 2006. Saccopastore 1: the earliest Neanderthal? A new look at an old cranium. In: Harvati K, Harrison T, editors. Neanderthals revisited: new approaches and perspectives. The Netherlands: Springer. p 23–36.

Bruner E, Manzi G. 2008. Paleoneurology of an early Neandertal: endocranial size, shape, and features of Saccopastore 1. J Hum E 54:729–742.

Bruner E, Pearson O. 2013. Neurocranial evolution in modern humans: the case of Jebel Irhoud 1. Anthropol Sci 121:31–41.

Bruner E, Manzi G, Arsuaga JL. 2003. Encephalization and allometric trajectories in the genus *Homo*: evidence from the Neandertal and modern lineages. Proc Natl Acad Sci USA 100:15335–15340.

Bruner E, Mantini S, Perna A, Maffei C, Manzi G. 2005. Fractal dimension of the middle meningeal vessels: variation and evolution in *Homo erectus*, Neanderthals, and modern humans. Eur J Morphol 42:217–224.

Bruner E, Grimaud-Hervé D, Wu XJ, de la Cuétara JM, Holloway R. 2015. A paleoneurological survey of *Homo erectus* endocranial metrics. Quat Int 368:80–87.

Buck LT, Stringer CB. 2014. *Homo heidelbergensis*. Curr Biol 26:R214–R215.

Collard M, Wood B. 2000. How reliable are human phylogenetic hypotheses? Proc Natl Acad Sci USA 97:5003–5006.

Dean D, Hublin JJ, Holloway R, Ziegler R. 1998. On the phylogenetic position of the pre-Neandertal specimen from Reilingen, Germany. J Hum E 34:485–508.

Gao B, Shen GJ, Qiu LC. 2007. Preliminary U-series dating of southern branch cave of Maba hominid site. J Jinan Univ (Nat Sci) 28:308–311.

Guangdong Museum. 1959. Brief report on the Maba human skull and associated animal fossils from Guangdong Province. Vertebr Palasiatica 2:94–96.

Gunz P, Neubauer S, Maureille B, Hublin JJ. 2010. Brain development after birth differs between Neanderthals and modern humans. Curr Biol 20:R921–R922.

Grimaud-Hervé D. 1997. L'évolution de l'enchéphale chez Homo erectus et Homo sapiens. Paris: CNRS Editions. p 1–420.

Gunz P, Mitteroecker P, Neubauer S, Weber GW, Bookstein FL. 2009. Principles for the virtual reconstruction of hominin crania. J Hum E 57:48–62.

Hammer Ø, Harper D, Ryan PD. 2001. PAST: Paleontological Statistics Software Package for education and data analysis. Palaeontol Electr 4:9–19.

Harvati K, Hublin JJ, Gunz P. 2010. Evolution of middle-late human cranio-facial form: a 3-D approach. J Hum E 59:445–464.

Hawks JD, Wolpoff MH. 2001. The accretion model of Neandertal evolution. Evolution 55:1474–1485.

Holloway RL. 1980. Within-species brain-body weight variability: a reexamination of the Danish Data and other primate species. Am J Phys Anthropol 53:109–121.

Holloway RL, Broadfiled DC, Yuan MS. 2004. The human fossil record, Vol. 3: Brain endocast. Hoboken: Wiley-Liss.

Hublin JJ. 2009. The origin of Neandertals. Proc Natl Acad Sci USA 106:16022–16027.

Jolliffe IT. 2002. Principal component analysis, 2nd ed. Berlin: Springer.

Krause J, Orlando L, Serre D, Viola B, Prüfer K, Richards MP, Hublin JJ, Hänni C, Derevianko AP, Pääbo S. 2007. Neanderthals in central Asia and Siberia. Nature 449:902–904.

Kubo D, Kono RT, Saso A, Mizushima S, Suwa G. 2008. Accuracy and precision of CT-based endocranial capacity estimations: a comparison with the conventional millet seed method and application to the Minatogawa 1 skull. Anthropol Sci 116: 77–85.

Liang Z, Li J. 1959. The Maba site survey and the primary observation on the Maba skull fossil. J Sun Yatsen Univ 1: 136–146.

Mounier A, Marchal F, Condemi S. 2009. Is *Homo heidelbergensis* a distinct species? New insight on the Mauer mandible. J Hum E 56:219–246.

Plavcan JM, Cope DA. 2001. Metric variation and species recognition in the fossil record. Evol Anthropol 10:204–222.

Prossinger H. 2008. Mathematical analysis techniques of frontal sinus morphology, with emphasis on *Homo*. Anat Rec 291: 1455–1478.

Prüfer K, Racimo F, Patterson N, Jay F, Sankararaman S, Sawyer S, Heinze A, Renaud G, Sudmant PH, de Filippo C, Li H, Mallick S, Dannemann M, Fu Q, Kircher M, Kuhlwilm M, Lachmann M, Meyer M, Ongyerth M, Siebauer M, Theunert C, Tandon A, Moorjani P, Pickrell J, Mullikin JC, Vohr SH, Green RE, Hellmann I, Johnson PL, Blanche H, Cann H, Kitzman JO, Shendure J, Eichler EE, Lein ES, Bakken TE, Golovanova LV, Doronichev VB, Shunkov MV17, Derevianko AP, Viola B, Slatkin M, Reich D, Kelso J, Pääbo S. 2014. The complete genome sequence of a Neanderthal from the Altai Mountains. Nature 505:43–49.

Pope GG. 1992. Craniofacial evidence for the origin of modern humans in China. Am J Phys Anthropol 35:243–298.

Reich D, Green RE, Kircher M, Krause J, Patterson N, Durand EY, Viola B, Briggs AW, Stenzel U, Johnson PL, Maricic T, Good JM, Marques-Bonet T, Alkan C, Fu Q, Mallick S, Li H, Meyer M, Eichler EE, Stoneking M, Richards M, Talamo S, Shunkov MV, Derevianko AP, Hublin JJ, Kelso J, Slatkin M, Pääbo S. 2010. Genetic history of an archaic hominin group from Denisova Cave in Siberia. Nature 468:1053–1060.

Rightmire GP. 1998. Human evolution in the Middle Pleistocene: the role of *Homo heidelbergensis*. Evol Anthropol 6:218–227.

Rightmire GP. 2008. *Homo* in the Middle Pleistocene: hypodigms, variation, and species recognition. Evol Anthropol 17: 8–21.

Rightmire GP. 2004. Brain size and encephalization in early to mid-Pleistocene *Homo*. Am J Phys Anthropol 124:109–123.

Sawyer S, Renaud G, Viola B, Hublin JJ, Gansauge MT, Shunkov MV, Derevianko AP, Prüfer K, Kelso J, Pääbo S. 2015. Nuclear and mitochondrial DNA sequences from two Denisovan individuals. Proc Natl Acad Sci USA 112:15696–15700.

Schwartz JH, Tattersall I. 2003. The human fossil record, Vol. 2. Cranial morphology of genus Homo (Africa and Asia). New York, Wiley-Liss.

Seidler H, Falk D, Stringer C, Wilfing H, Mueller GB, Nedden DZ, Weber GW, Reicheis W, Arsuaga JL. 1997. A comparative study of stereolithographically modelled skulls of Petralona and Broken Hill: implications for future studies of Middle Pleistocene hominid evolution. J Hum E 33:691–703.

Shen GJ, Tu H, Xiao DF, Qiu LC, Feng YX, Zhao JX. 2014. Age of Maba hominin site in southern China: evidence from U-series dating of Southern Branch Cave. Quat Geochronol 23: 56–62.

Stringer CB. 2012. The status of *Homo heidelbergensis* (Schoetensack 1908). Evol Anthropol 21:101–107.

Tattersall I. 1986. Species recognition in human paleontology. J Hum E 15:165–175.

Woo RK, Peng RC. 1959. Fossil human skull of early Paleoanthropic stage found at Mapa, Shaoquan, Kwantung Province. Vertebrata Palasiatica 3:176–182.

Wu XZ. 1988. Comparative study of early *Homo sapiens* from China and Europe. Acta Anthropol Sin 7:292–299.

Wu XJ. 2004. On the origin of modern humans in China. Quat Int 117:131–140.

Wu XJ, Trinkaus E. 2014. The Xujiayao 14 mandibular ramus and Pleistocene *Homo* mandibular variation. Comp Rendus Pale 13:333–341.

Wu XJ, Schepartz L, Liu W. 2010a. Endocranial Cast of Zhoukoudian Skull V: A New *Homo erectus* brain endocast from China. Proc R Soc B 277:337–344.

Wu XJ, Schepartz L, Norton CJ. 2010b. Morphological and morphometric analysis of variation in the Zhoukoudian *Homo erectus* brain endocasts. Quat Int 211:4–13.

Wu XJ, Crevecoeur I, Liu W, Xing S, Trinkaus E. 2014. The temporal labyrinths of eastern Eurasian Pleistocene humans. Proc Natl Acad Sci USA 111:10509–10513.

Xing S, Martinón-Torres M, Bermúdez de Castro JM, Wu XJ, Liu W. 2015. Hominin teeth from the early Late Pleistocene site of Xujiayao, Northern China. Am J Phys Anthropol 156: 224–240.

Xiao D, Bae CJ, Shen G, Delson E, Jin JJH, Webb NM, Qiu L. 2014. Metric and geometric morphometrics analysis of new hominin fossils from Maba (Guangdong, China). J Hum E 74: 1–20.

Xu CH, Huang ZG. 1988. Geological age of Maba man and related problem. In: Guangdong Provincial Museum and the Museum of the Qujiang County, editor. Treatise in Commemoration of the 30th Anniversary of the Discovery of Maba Human Cranium. Beijing: Cultural Relics Publishing House Press. p 36–42.

Yuan S, Chen T, Gao S. 1986. Uranium series chronological sequence of some Paleolithic sites in south China. Acta Anthropol Sin 5:179–190.

Zollikofer CPE, Weissmann JD. 2008. A morphogenetic model of cranial pneumatization based on the invasive tissue hypothesis. Anat Rec 291:1446–1454.